

# A direct *ab initio* dynamics approach for calculating thermal rate constants using variational transition state theory and multidimensional semiclassical tunneling methods. An application to the $\text{CH}_4 + \text{H} \leftrightarrow \text{CH}_3 + \text{H}_2$ reaction

Thanh N. Truong

Department of Chemistry, University of Utah, Salt Lake City, Utah 84112

(Received 6 December 1993; accepted 17 February 1994)

We present a new methodology, called "direct *ab initio* dynamics," for calculations of thermal rate constants and related properties from first principles. The new method is based on full variational transition state theory plus multidimensional semiclassical tunneling transmission coefficients with the potential energy information to be calculated from an accurate level of *ab initio* electronic structure theory. To make this approach practical, we propose the use of a focusing technique to minimize the number of electronic structure calculations, while still preserving the accuracy of the dynamical results. We have applied this method to study detailed dynamics of the hydrogen abstraction reaction,  $\text{CH}_4 + \text{H} \leftrightarrow \text{CH}_3 + \text{H}_2$ , and obtained excellent agreement with the available experimental data for both the forward and reverse rate constants for a range of temperatures from 300 to 1500 K. In these calculations, the potential energy surface was calculated at the quadratic configuration interaction including single and double excitation (QCISD) level of theory using the triple-zeta plus polarizations 6-311G(*d,p*) basis set.

## I. INTRODUCTION

The prediction of reaction rates from first principles is a major goal and has been one of the grand challenges in theoretical chemistry. For this reason, direct dynamics methods recently has been received great attention.<sup>1-29</sup> In the direct dynamics approach, all required energies and forces for each geometry that is important for evaluating dynamical properties are obtained directly from electronic structure calculations. The main advantage of this approach is that it eliminates the need of an accurate analytical potential energy function (PEF) used in many conventional dynamical methods. The development of such an analytical potential energy function is not a trivial task, particularly in the design of its functional form, and even having fitted the functional form to available experimental or accurate theoretical information, no rule exists for ensuring the correct global topology. Hence, direct dynamics approach offers an alternative if not only for dynamical studies of complex systems. Our contributions to this area recently include the development of two new methodologies for calculating thermal rate constants and related properties. One approach is to estimate thermal rate constants and tunneling contribution using the interpolated variational transition state theory (VTST) models<sup>20,23,24</sup> when limited accurate *ab initio* electronic structure information is available. Difficulties, such as mode crossing, however, often arise when one attempts to interpolate limited information in the region near the saddle point to the reactants and products. The other approach<sup>22,25,28,29</sup> is to carry out full VTST calculations<sup>28,30-35</sup> with multidimensional semiclassical tunneling approximations using the semiempirical molecular orbital Hamiltonians at the neglect diatomic differential overlap (NDDO) level<sup>36-38</sup> with specific reaction parameters. In this approach we use the semiempirical molecular orbital Hamiltonian entirely as a fitting function with parameters

fitted to accurate *ab initio* molecular orbital (MO) results or experimental data for a specific reaction. This approach has been successfully applied to various chemical reactions and has shown considerable promise.<sup>22,25,28,29</sup> However, adjusting the original NDDO parameters, such as AM1 or PM3, is not always a simple task, particularly when the original NDDO potential energy surface differs significantly from the reference accurate *ab initio* one. Furthermore, adjusting the NDDO parameters undoubtedly modifies the electronic properties of the system calculated from the wave function such as the electrostatic potential, dipole moment, etc. Though these properties are not needed for dynamical calculations, they are sometimes of interest as functions of the reaction coordinate.

In the present paper, we present a new methodology, called "direct *ab initio* dynamics" that allows studies of detailed dynamics of chemical reactions from first principles. This method is based on a full variational transition state theory<sup>30-34,39-54</sup> plus multidimensional semiclassical adiabatic ground-state tunneling approximations<sup>30-35</sup> with the potential energy information to be calculated directly from a sufficiently accurate level of *ab initio* molecular orbital theory. To make this approach practical for complex systems, we introduce a focusing technique to minimize the number of electronic structure calculations while preserving the accuracy of the dynamical results. To illustrate the applicability of the new method, we have applied it to study detailed reactive dynamics of a fundamentally important reaction, namely the  $\text{CH}_4 + \text{H} \leftrightarrow \text{CH}_3 + \text{H}_2$  reaction.

The reaction  $\text{CH}_4 + \text{H} \leftrightarrow \text{CH}_3 + \text{H}_2$  and its reverse have served as a prototype reaction involving polyatomic molecules and have played an important role in the theoretical and experimental development of chemical kinetics.<sup>55,56</sup> In addition to their intrinsic importance to combustion kinetics, they are of fundamental interest to organic reaction mecha-

nisms. For this reason, CH<sub>4</sub>+H reaction has been the subject of intense theoretical and experimental investigations.

Experimentally, the abstraction reaction CH<sub>4</sub>+H'↔CH<sub>3</sub>+HH' has been observed as the dominant process at low energies with the activation energy of 11.8 kcal/mol. However, the exchange reaction CH<sub>4</sub>+H'↔H'CH<sub>3</sub>+H also occurs at high energies with the threshold of the order 3 kcal/mol. Due to its importance and advances in experimental methods, thermal rate constants for both the forward and reverse reactions of CH<sub>4</sub>+H↔CH<sub>3</sub>+H<sub>2</sub> have been remeasured several times by different groups<sup>57-88</sup> in the past and are generally with a good reproducibility especially for the forward reaction. For the reverse reaction, the agreement is not as good.

Theoretically, there have been numerous studies of the CH<sub>4</sub>+H↔CH<sub>3</sub>+H<sub>2</sub> reaction to examine its potential energy surface (PES) by both *ab initio* electronic structure calculations and semiempirical treatments of the global PES, and to model its detailed dynamics by trajectory and semiclassical variational transition state theory (VTST) calculations. We briefly mention only the recent studies here.

The most accurate *ab initio* calculations to date were from the work of Kraka, Gauss, and Cremer<sup>89</sup> using the couple cluster method which includes single and double excitations with a perturbative treatment of triple excitations, CCSD(T) with a quadruple zeta plus polarization basis set. Two earlier works were from Walch and co-workers<sup>90-92</sup> using the polarization configuration interaction (Pol-CI) method and from Schlegel and co-workers<sup>93</sup> using the spin projected Möller–Plesset perturbation theory. These studies computed the geometries and vibrational frequencies of the transition state and equilibrium structures, and the barrier height for the abstraction reaction. Subsequently, the results were then used to calculate the forward and reverse rate constants using conventional transition state theory (TST) with Wigner's lowest-order tunneling correction (TST/W). Note that the Wigner's correction is only valid near the saddle point region, however, more accurate treatments for tunneling require more information on the PES.

Although the development of semiempirical analytical global PEF is a laborious task, there exists three sets of analytical PEF's which incorporate all degrees of freedom for the CH<sub>4</sub>+H↔CH<sub>3</sub>+H<sub>2</sub> reaction. The earlier two PEF's developed originally by Raff<sup>94</sup> and by Bunker and co-workers<sup>95</sup> to model both the abstraction and exchange reactions have been used for trajectory calculations. The later PEF's known as *J1*, *J2*, and *J3* were introduced by Truhlar and co-workers.<sup>96</sup> These PEF's were calibrated to *ab initio* electronic structure results, experimental thermochemical data, vibrational frequencies, reaction rate constants, Arrhenius parameters, and kinetic isotope effects (KIE) for the abstraction reaction only, and have been used with variational transition state theory to study temperature dependencies of the thermal rate constants and kinetic isotope effects of the abstraction reaction.<sup>96,97</sup>

Although the *J1*, *J2*, and *J3* PEF's have fixed many deficiencies pointed out by Steckler *et al.*<sup>98</sup> in the earlier two PEF's, there is still an uncertainty in the barrier width that may result from the accuracy of the semiclassical tunneling method which was used to calibrate them. In the present

study, since the potential energy surface is calculated at a sufficiently accurate level of *ab initio* electronic structure theory, particularly at the quadratic configuration interaction including single and double excitation (QCISD) level<sup>99</sup> of theory with the triple zeta plus polarization 6-311G(*d,p*) basis set,<sup>100</sup> the present results should provide information which may be compared with the results from the previous analytical PEF's and which may be used to calibrate more accurate PEF's for future trajectory simulations where potential information if calculated directly at the same level of accuracy may still be prohibitively expensive.

In Sec. II, we give an overview of the methodologies for both the VTST and multidimensional semiclassical tunneling methods used in this study. Computational details for electronic structure calculations of the minimum energy path information and for VTST calculations are given in Sec. III. The results and discussion are given in Sec. IV. Finally, a summary of the present study is given in Sec. V.

## II. THEORY

### A. Variational transition state theory

Variational transition state theory is based on the idea that by varying the dividing surface along a reference path to minimize the rate, one can minimize the error due to "re-crossing" trajectories. In the present study, the reference path is the minimum energy path (MEP) which is defined as the steepest descent path from the saddle point to both the reactant and product directions in the mass-weighted Cartesian coordinate system. Most previous applications of VTST however were done in the mass-scaled Cartesian coordinate system. It is important to point out that the choice between the mass-weighted or mass-scaled Cartesian coordinate system has absolutely *no* effects on the calculated observables. It is merely for the conveniences in interpreting the intermediate results. Moreover, if we choose the reduced mass,  $\mu$ , to be 1 amu in the mass-scaled Cartesian coordinate system, then both the mass-weighted and mass-scaled coordinate systems yield numerically identical intermediate results. The reaction coordinate  $s$  is then defined as the distance along the MEP with the origin located at the saddle point and is positive on the product side and negative on the reactant side. For a canonical ensemble at a given temperature  $T$ , the canonical variational theory (CVT) rate constant for a bimolecular reaction is given by<sup>30-34,46,47</sup>

$$k^{\text{CVT}}(T) = \min_s k^{\text{GT}}(T, s), \quad (1)$$

where

$$k^{\text{GT}}(T, s) = \frac{\sigma}{\beta h} \frac{Q^{\text{GT}}(T, s)}{\Phi^{\text{R}}(T)} e^{-\beta V_{\text{MEP}}(s)}. \quad (2)$$

In these equations,  $k^{\text{GT}}(T, s)$  is the generalized transition state theory rate constant at the dividing surface which intersects the MEP at  $s$  and is orthogonal to the MEP at the intersection point.  $\sigma$  is the symmetry factor accounting for the possibility of more than one symmetry-related reaction path. For the CH<sub>4</sub>+H↔CH<sub>3</sub>+H<sub>2</sub> reaction,  $\sigma$  equals to 4 for both the forward and reverse directions.  $\beta$  is  $(k_b T)^{-1}$ , where

$k_b$  is the Boltzmann's constant;  $h$  is the Planck's constant.  $\Phi^R(T)$  is the reactant partition function (per unit volume for bimolecular reactions).  $V_{\text{MEP}}(s)$  is the classical potential energy (also called the Born–Oppenheimer potential) along the MEP with its zero of energy at the reactants, and  $Q^{\text{GT}}(T,s)$  is the internal partition function of the generalized transition state at  $s$  with the local zero of energy at  $V_{\text{MEP}}(s)$ . Both  $\Phi^R(T)$  and  $Q^{\text{GT}}(T,s)$  partition functions are approximated as products of electronic, vibrational, and rotational partition functions. For the electronic partition function, the generalized transition state electronic excitation energies and degeneracies are assumed to be the same as at the transition state. For the reaction studied here, we assume that there are no low-lying excited states at the saddle point. For rotations, since the rotational energy levels are generally closely spaced, little accuracy is lost if we approximate the quantal rotational partition functions by the classical ones. For vibrations, in the present study, the partition functions are calculated quantum mechanically within the framework of the harmonic approximation. Thus, canonical variational transition state theory yields the hybrid (i.e., classical reaction path motion with other degrees of freedom quantized) rate constants. Furthermore, if the generalized transition state is located at the saddle point ( $s=0$ ), Eq. (2) reduces to the conventional transition state theory.

To include quantal effects for motion along the reaction coordinate, we multiply CVT rate constants by a ground-state transmission coefficient,  $\kappa^{\text{CVT/G}}(T)$ . Thus, the final quantized rate constant is

$$k^{\text{CVT/G}}(T) = \kappa^{\text{CVT/G}}(T) k^{\text{CVT}}(T). \quad (3)$$

## B. Multidimensional semiclassical tunneling methods

First, we approximate the effective potential for tunneling to be the vibrationally adiabatic ground-state potential curve defined by

$$V_a^G(s) = V_{\text{MEP}}(s) + \epsilon_{\text{int}}^G(s), \quad (4)$$

where  $\epsilon_{\text{int}}^G(s)$  denotes the zero-point energy in vibrational modes transverse to the MEP. The ground state transmission coefficient,  $\kappa^{\text{CVT/G}}(T)$ , is then approximated as the ratio of the thermally average multidimensional semiclassical ground-state transmission probability,  $P^G(E)$ , for reaction in the ground state to the thermally average classical transmission probability for one-dimensional scattering by the ground-state effective potential  $V_a^G(s)$ .<sup>28,30–35,101–104</sup> If we denote the CVT transition state for temperature  $T$  as  $s_*^{\text{CVT}}(T)$ , the value of  $V_a^G\{s_*^{\text{CVT}}(T)\}$ , denoted as  $E_*(T)$ , is the quasiclassical ground-state threshold energy. Then

$$\kappa^{\text{CVT/G}}(T) = \frac{\int_0^\infty P^G(E) e^{-E/k_b T} dE}{\int_{E_*(T)}^\infty e^{-E/k_b T} dE}. \quad (5)$$

Notice that the integral in the numerator of Eq. (5) involves  $E$  above  $E_*(T)$ , as well as tunneling energies below this. Thus, semiclassical transmission probability  $P^G(E)$  accounts for both nonclassical reflection at energies above the quasiclassical threshold and also nonclassical transmission, i.e.,

tunneling, at energies below that threshold. Though, because of the Boltzmann factor in Eq. (5), tunneling is by far the more important of the two effects.

Several approximations for the semiclassical transmission probability  $P^G(E)$  are available, however, only two, namely, the zero-curvature<sup>32</sup> and the centrifugal-dominant small-curvature semiclassical adiabatic ground-state<sup>35</sup> approximations used in the present study are presented here. For convenience, we labeled them as ZCT and SCT for the zero-curvature tunneling and small-curvature tunneling cases, respectively. Since the zero-curvature tunneling (ZCT) approximation is a special case of the small-curvature tunneling (SCT) approximation, we present only the formalism for the SCT below.

The centrifugal-dominant small-curvature semiclassical adiabatic ground-state approximation (SCT) is a generalization of the Marcus–Coltrin approximation in which the tunneling path is distorted from the MEP out to a concave-side vibrational turning point in the direction of the internal centrifugal force. Instead of defining the tunneling path, the centrifugal effect is included by replacing the reduced mass by an effective reduced mass,  $\mu_{\text{eff}}(s)$ , which is used to evaluate imaginary action integrals and thereby tunneling probabilities. Note that in the mass-weighted Cartesian coordinate system, the reduced mass  $\mu$  is set equal to 1 amu. The ground-state transmission probability at energy  $E$  is

$$P^G(E) = \frac{1}{\{1 + e^{-2\theta(E)}\}}, \quad (6)$$

where  $\theta(E)$  is the imaginary action integral evaluated along the tunneling path,

$$\theta(E) = \frac{2\pi}{h} \int_{s_l}^{s_r} \sqrt{2\mu_{\text{eff}}(s) |E - V_a^G(s)|} ds \quad (7)$$

and where the integration limits,  $s_l$  and  $s_r$ , are the reaction-coordinate turning points defined by

$$V_a^G[s_l(E)] = V_a^G[s_r(E)] = E. \quad (8)$$

Note that the ZCT results can be obtained by setting  $\mu_{\text{eff}}(s)$  equal to  $\mu$  in Eq. (7). The effect of the reaction-path curvature included in the effective reduced mass  $\mu_{\text{eff}}(s)$  is explained below.

The small-curvature tunneling amplitude corresponds approximately to an implicit tunneling path that follows the line of concave-side vibrational turning point at a distance  $\bar{t}(s)$  from the MEP in the direction of the reaction-path curvature vector. Let the distance along the small-curvature tunneling path be  $\xi$  and the curvature at  $s$  be  $\kappa(s)$ ; then it can be shown by analytical geometry that

$$d\xi = \sqrt{\left[ [1 - \bar{a}(s)]^2 + \left[ \frac{d\bar{t}(s)}{ds} \right]^2 \right]} ds, \quad (9)$$

where

$$\bar{a}(s) = |\kappa(s)\bar{t}(s)|. \quad (10)$$

The imaginary action integral along the small-curvature tunneling path is defined as

$$\theta(E) = \frac{2\pi}{h} \int \sqrt{2\mu[E - V_a^G[s(\xi)]]} d\xi. \quad (11)$$

By comparing Eqs. (7) and (11), the effective reduced mass is given by

$$\mu_{\text{eff}}(s) = \mu \left\{ [1 - \bar{a}(s)]^2 + \left[ \frac{d\bar{t}(s)}{ds} \right]^2 \right\}. \quad (12)$$

However, to make the method generally applicable even when  $\bar{t}(s)$  is greater than or equal to the radius of curvature of the reaction path, we include only the leading terms of Eq. (12) but not singularities by the approximated form below

$$\mu_{\text{eff}}(s) = \mu \times \min \left\{ \frac{\exp\{-2\bar{a}(s) - [\bar{a}(s)]^2 + (d\bar{t}/ds)^2\}}{1} \right\}. \quad (13)$$

The magnitude of the reaction-path curvature  $\kappa(s)$  is given by

$$\kappa(s) = \left\{ \sum_{m=1}^{F-1} [\kappa_m(s)]^2 \right\}^{1/2}, \quad (14)$$

where the summation is over all generalized normal modes ( $m=1,2,3,\dots,F-1$ ), and  $\kappa_m(s)$  is the reaction-path curvature component along mode  $m$  given by<sup>105</sup>

$$\kappa_m(s) = -\mathbf{L}_m^T \mathbf{F} \frac{\nabla V}{|\nabla V|^2}, \quad (15)$$

and where  $\mathbf{L}_m^T$  is the transpose of the generalized normal mode eigenvector of mode  $m$ ,  $\mathbf{F}$  is the force constant matrix (Hessian matrix),  $\nabla V$  is the gradient. Finally, within the harmonic approximation,  $\bar{t}(s)$  is given by

$$\bar{t}(s) = \left( \frac{\kappa \hbar}{\mu} \right)^{1/2} \left\{ \sum_m^{F-1} [\kappa_m(s)]^2 w_m^2(s) \right\}^{-1/4}, \quad (16)$$

where  $w_m$  is the generalized vibrational frequency of mode  $m$ . Equivalently, Eq. (10) may be rewritten as

$$\bar{a}(s) = \kappa^{3/2} \left( \frac{\hbar}{\mu} \right)^{1/2} \left\{ \sum_m^{F-1} [\kappa_m(s)]^2 w_m^2(s) \right\}^{-1/4}. \quad (17)$$

### III. COMPUTATIONAL DETAILS

#### A. Electronic structure calculations

First, we need to determine the level of electronic structure theory and the basis set that would give sufficient accurate potential information needed for the VTST rate calculations and yet computationally feasible. For this purpose, we have employed two correlated levels of theory, namely the second order Møller–Plesset perturbation theory<sup>106</sup> (MP2) and the quadratic configuration interaction including single and double substitutions (QCISD) (Ref. 99) using two different basis sets, namely the triple-zeta plus polarization 6-311G(*d,p*),<sup>100</sup> and Dunning's correlation-consistent polarized valence double-zeta [3*s2p1d/2s1p*] basis set,<sup>107</sup> denoted as cc-pVDZ. Particularly, we have examined the accuracy of each level/basis for predicting the H<sub>3</sub>C–H and H–H bond energies with special attention given to the balance in the treatment of electron correlation in both of these bonds,

the equilibrium and transition state structures, the reaction endoergicity, and classical barrier height of the abstraction reaction by comparisons with the available experimental data. We have also compared these results with those from more accurate *ab initio* calculations of Kraka *et al.*,<sup>89</sup> particularly at the CCSD(T) level of theory using Dunning's correlated consistent valence quadruple zeta [5*s4p3d/4s3p*], denoted as (cc-VQZ), basis set.

For the MP2 calculations, gradients and Hessians were calculated analytically, whereas for the QCISD calculations only gradients were calculated analytically while Hessians were calculated numerically. To estimate the error in the calculated QCISD Hessians resulting from the central difference procedure, we examined the eigenvalues of the translational and rotational modes at the transition state and found them to be less than 20 cm<sup>-1</sup> indicating that such error is acceptably small. However, as the MEP approaches the reactant or product region, this error is expected to increase somewhat, though the VTST calculations are not very sensitive to these regions.

Having determined the level/basis of electronic structure method for VTST calculations, the minimum energy path was then calculated in the mass-weighted internal coordinates using the second order Gonzalez and Schlegel<sup>108</sup> method with a stepsize of 0.1 (amu)<sup>1/2</sup> bohr. It was reported that this method gives nearly the identical MEP for integrating in the mass-weighted Cartesian and mass-weighted internal coordinates, and also yields the correct tangent and curvature vectors in the limit of small step sizes.<sup>108</sup>

All electronic structure calculations were done using the GAUSSIAN92 program.<sup>109</sup>

#### B. Variational transition state theory and semiclassical tunneling calculations

In this study, we introduced the use of a focusing technique to assure the convergence of the calculated rate constants with a minimal number of Hessian calculations. This was done by first carrying out the preliminary rate calculations with coarse Hessian grids to estimate regions containing the temperature dependent canonical transition states,  $s_*^{\text{CVT}}(T)$ , and the minima of the effective reduced mass where the “corner cutting” effect would be largest. The finer grids were then calculated for these critical regions to improve the accuracy of the calculated canonical rate constants and small-curvature tunneling probability. This approach allows us to obtain the optimal accuracy for a given computational resource. For the title reaction, the total of 21 Hessian unstructured grid points was needed.

The canonical transition state, i.e., the location of the maximum of the free-energy of activation, for given temperature was determined by a quadratic-quartic fit. The remaining quantity that depends on the Hessian grid size is the derivative of the vibrational turning point with respect to the reaction coordinate used in calculating the effective reduced mass as shown in Eq. (13). This derivative was calculated from the sixth order Lagrangian interpolations of the vibrational turning points as a function of the reaction coordinate.

The present methodology for VTST and small-curvature

TABLE I. Equilibrium structures (distances are in Å).

Level	$R_{\text{C-H}}(\text{CH}_4)$	$R_{\text{C-H}}(\text{CH}_3)$	$R_{\text{H-H}}(\text{H}_2)$
MP2/6-311G( <i>d,p</i> )	1.090	1.079	0.738
MP2/cc-pVDZ	1.098	1.088	0.753
QCISD/6-311G( <i>d,p</i> )	1.093	1.083	0.743
QCISD/cc-pVDZ	1.101	1.092	0.761
CCSD(T)/cc-VQZ <sup>a</sup>	1.086	1.076	0.741
Expt. <sup>b</sup>	1.086	1.076	0.741

<sup>a</sup>Reference 89.<sup>b</sup>References 111 and 112.

tunneling calculations was implemented in our new DIRATE (direct rate) program.<sup>110</sup>

## IV. RESULTS AND DISCUSSIONS

### A. Reactants and products

#### 1. Geometries

The optimized bond lengths of methane, methyl, and hydrogen molecules are given in Table I. We found that the 6-311G(*d,p*) is more accurate than the cc-pVDZ basis set when used with the MP2 or QCISD level to predict these equilibrium structures. Particularly, MP2 and QCISD calculations using the cc-pVDZ basis set predict bond lengths too large in all cases compared to the experimental data<sup>111,112</sup> and accurate CCSD(T)/cc-VQZ results<sup>89</sup> with the maximum error of 0.02 Å. Using the 6-311G(*d,p*) basis set, MP2 and QCISD calculations, however, yield better agreement with the maximum error of 0.007 Å.

#### 2. Bond energies

The calculated bond energies,  $D_e$  as  $E(\text{R-H}) - E(\text{R}) - E(\text{H})$ , for the  $\text{H}_3\text{C-H}$  and  $\text{H-H}$  bonds and the experimental values<sup>111,112</sup> are given in Table II. In the present study, we found that both the MP2 and QCISD levels underestimate bond energies for both the  $\text{H}_3\text{C-H}$  and  $\text{H-H}$  bonds. In particular, the UMP2 level yields the errors of 4.0 and 8.6 kcal/mol or 3.6% and 8.0% for the  $\text{CH}_3\text{-H}$  and  $\text{H-H}$  bonds, respectively, if using the 6-311G(*d,p*) basis set, and of 5.3 and 10.7 kcal/mol or 4.7% and 9.8%, respectively, if using the cc-pVDZ basis set. Projecting out the spin contamination in the MP2 wave function of the methyl radical further worsens the result for  $D_e(\text{CH}_3\text{-H})$ . The QCISD calculations yield better bond energies. For instance,  $D_e(\text{CH}_3\text{-H})$  and

TABLE II. Calculated  $D_e$  bonding energies (kcal/mol) for  $\text{CH}_4$  and  $\text{H}_2$ .

Level	$D_e(\text{H}_3\text{C-H})$	%Error	$D_e(\text{H-H})$	%Error
Expt. <sup>a</sup>	112.1	0.0	109.6	0.0
MP2/6-311G( <i>d,p</i> )	108.1(106.7) <sup>b</sup>	3.6(4.8)	100.8	8.0
MP2/cc-pVDZ	106.8(105.6)	4.7(5.8)	98.9	9.8
QCISD/6-311G( <i>d,p</i> )	108.6	3.1	106.1	3.2
QCISD/cc-pVDZ	106.7	5.0	104.2	4.8
CCSD(T)/cc-VQZ <sup>c</sup>	110.7	1.2	107.9	1.5

<sup>a</sup>References 111 and 112.<sup>b</sup>Values in parentheses are from spin projected MP2 at the UMP2/6-311G(*d,p*) geometries.<sup>c</sup>Reference 89.

$D_e(\text{H-H})$  are underestimated both by 3.5 kcal/mol, or 3.1% and 3.2% error, respectively, using the 6-311G(*d,p*) basis set, whereas the errors are larger and of the order 5% using the cc-pVDZ basis set. These results can be compared with the previous CCSD(T)/cc-VQZ calculations from Kraka *et al.*<sup>89</sup> which predicted bond energies for both bonds accurate within 1.5% error. Furthermore, notice that between the MP2 and QCISD levels, the QCISD level has better balance in the treatment of electron correlation in both  $\text{H}_3\text{C-H}$  and  $\text{H-H}$  bonds as indicated by the same order of error in the calculated bond energies. As discussed below, such correlation balance yields better predictions of reaction energetics for reactions involving these bonds. The importance of correlation balance in predictions of reaction energetics also had been discussed previously.<sup>113</sup>

### 3. Vibrational frequencies

The harmonic frequencies and zero-point energies for methane, methyl, and hydrogen from the present MP2 and QCISD calculations using the 6-311G(*d,p*) basis set are given in Table III. For comparisons, we also listed in Table III results from the previous CCSD(T) study<sup>89</sup> and analytical PEF *J3*,<sup>96</sup> and the experimental data.<sup>111,112</sup> We found that with the exception of the out-of-plane  $a''$  bending mode of the methyl radical, all three levels of theory, MP2, QCISD, and CCSD(T), generally overestimate the harmonic frequencies in all modes, though the QCISD and CCSD(T) results are in better agreement with the experimental data. The methyl out-of-plane  $a''$  bending frequency is noticeably underestimated by all three levels, particularly, the errors of the order 162, 148, and 88  $\text{cm}^{-1}$  for the MP2, QCISD, CCSD(T) levels, respectively. Furthermore, the present QCISD/6-311G(*d,p*) calculations yield vibrational frequencies for the equilibrium structures quantitatively similar to the results from the previous CCSD(T)/cc-VQZ calculations<sup>89</sup> which are computationally more expensive with the maximum difference of the order 60  $\text{cm}^{-1}$ .

### B. Saddle point

#### 1. Geometry

From Table IV, we can compare the  $C_{3v}$  saddle point geometry obtained from the present MP2 and QCISD calculations with those from the previous CCSD(T) study<sup>89</sup> and the analytical PEF *J3*.<sup>96</sup> Since the spectator C-H bonds and the H-C-H<sub>a</sub> angle do not differ significantly for different surfaces, we focus only on the two C-H<sub>a</sub> and H<sub>a</sub>-H active bonds, as listed in the second and third columns in Table IV. We found that there are noticeable differences up to 0.07 Å in these bond lengths for different potential energy surfaces. If we use the CCSD(T)/cc-VQZ geometry as a reference point on the reaction path where the C-H<sub>a</sub> and H<sub>a</sub>-H bonds are stretched by 0.30 and 0.16 Å, respectively, from their equilibrium bond lengths, we found that the QCISD/6-311G(*d,p*) saddle point is very close to the reference point with the maximum difference in the active bond lengths of less than 0.003 Å, whereas the *J3* saddle point is noticeably shifted toward the reactant  $\text{CH}_4 + \text{H}$  side, and the MP2 ones are shifted toward the product  $\text{CH}_3 + \text{H}_2$  side.

TABLE III. Harmonic frequencies (cm<sup>-1</sup>) and zero-point energies (kcal/mol) for the reactant and products.

Modes	MP2/ 6-311G( <i>d,p</i> )	QCISD/ 6-311G( <i>d,p</i> )	CCSD(T) <sup>a</sup> cc-VQZ	<i>J3</i> <sup>b</sup>	Expt. <sup>c</sup>
CH <sub>3</sub>					
<i>a'</i>	3173	3128	3125	2986	3002
<i>a''</i>	418	432	492	580	580
<i>e</i>	3366	3310	3307	3173	3184
<i>e</i>	1447	1436	1445	1383	1383
ZPE	18.9	18.7	18.8	18.1	18.2
CH <sub>4</sub>					
<i>a<sub>1</sub></i>	3076	3047	3037	2876	2917
<i>e</i>	1580	1573	1592	1505	1534
<i>t<sub>1</sub></i>	3213	3167	3153	3039	3019
<i>t<sub>2</sub></i>	1364	1367	1366	1344	1306
ZPE	28.5	28.3	28.3	27.2	27.1
H <sub>2</sub>					
$\Sigma_g$	4533	4422	4409	4401	4401
ZPE	6.5	6.4	6.3	6.3	6.3

<sup>a</sup>Reference 89.<sup>b</sup>Reference 96.<sup>c</sup>JANAF tables (Ref. 111).

## 2. Vibrational frequencies

Normal mode analyses at the saddle point were carried out at the MP2 and QCISD levels of theory using the 6-311G(*d,p*) basis set. The resulting harmonic frequencies are listed in Table V with those from the previous CCSD(T) calculations,<sup>89</sup> and the *J3* analytical PEF.<sup>96</sup> Compared to the *J3* frequencies, all three *ab initio* levels, MP2, QCISD, and CCSD(T), yield a similar trend. Particularly, frequencies with the magnitude larger than 1250 cm<sup>-1</sup> are slightly overestimated whereas bending frequencies with the magnitude less than 1250 cm<sup>-1</sup> are underestimated by at most 12%. Overall, the QCISD and CCSD(T) real frequencies are noticeably closer to the *J3* ones than the MP2. The imaginary frequency, however, is noticeably larger in all *ab initio* surfaces, particularly with the magnitude of 1639, 1529, and 1500 *i* cm<sup>-1</sup> for the MP2, QCISD, and CCSD(T) surfaces, respectively, as compared to the *J3* value of 1088 *i* cm<sup>-1</sup>. This may indicate that the *J3* PEF has a wider barrier width or the *ab initio* surfaces have steeper MEP's which can be due to having higher classical barriers as discussed below. It is also important to point out that the present QCISD/6-311G(*d,p*) calculations also yield transition state vibrational frequencies quantitatively similar to the previous CCSD(T)/cc-VQZ calculations<sup>89</sup> with the maximum difference of the order 30 cm<sup>-1</sup>.

TABLE IV. Transition state structure (distances are in Å, angle is in deg).

Level	<i>R</i> <sub>CH</sub>	<i>R</i> <sub>HH</sub>	<i>R</i> <sub>CH'</sub>	Alpha
MP2/6-311G( <i>d,p</i> )	1.409	0.873	1.086	103.2
MP2/cc-pVDZ	1.426	0.882	1.094	102.7
QCISD/6-311G( <i>d,p</i> )	1.390	0.899	1.089	103.7
QCISD/cc-pVDZ	1.407	0.910	1.097	103.2
CCSD(T)/cc-VQZ <sup>a</sup>	1.393	0.897	1.082	103.2
<i>J3</i> <sup>b</sup>	1.37	0.94	1.08	103.1

<sup>a</sup>Reference 89.<sup>b</sup>Reference 96.

## C. Reaction energetics

The reaction energetics information is given in Table VI including results from the present MP2 and QCISD calculations, and from the previous MP4 (Ref. 93) and CCSD(T) (Ref. 89) calculations, the analytical *J3* PEF (Ref. 96) and the experimental data. First, notice that both the present spin projected PMP2 and the previous PMP4 results overestimate the reaction endoergicity by 2.3 and 0.6 kcal/mol, respectively. Due to having better correlation balance, the QCISD and CCSD(T) calculations predict the endoergicity of 2.5 and 2.8 kcal/mol, respectively, that is closer to the experimental value of 2.6 kcal/mol. Adding the zero-point energy contribution, both the present QCISD/6-311G(*d,p*) and the previous CCSD(T)/cc-VQZ calculations<sup>89</sup> predict the reaction is exothermic by 0.7 and 0.4 kcal/mol at 0 K, respectively. This is close to the widely accepted view that the reaction is thermal neutral with the experimental heat of reaction,  $\Delta H_0^0$ , of -0.02 kcal/mol as reported in the JANAF tables.<sup>111</sup> However, it is interesting to point out that in contrast to this view, recent TST fit to the experimental rates by Furue and Pacey<sup>114</sup> yielded  $\Delta H_0^0$  to be of the order -1.3

TABLE V. Harmonic frequencies (cm<sup>-1</sup>) and zero-point energies (kcal/mol) for the transition state of the CH<sub>4</sub>+H $\leftrightarrow$ CH<sub>3</sub>+H<sub>2</sub> reaction.

Modes	UMP2	QCISD	CCSD(T) <sup>a</sup>	<i>J3</i> <sup>b</sup>
<i>a<sub>1</sub></i>	3125	3090	3083	3006
<i>a<sub>1</sub></i>	1958	1764	1763	1711
<i>a<sub>1</sub></i>	1093	1111	1093	1248
<i>e</i>	3287	3236	3229	3068
<i>e</i>	1463	1459	1458	1376
<i>e</i>	1142	1152	1124	1202
<i>e</i>	544	534	518	586
<i>a<sub>1</sub></i>	1639 <i>i</i>	1529 <i>i</i>	1500 <i>i</i>	1088 <i>i</i>
ZPE	27.2	26.8	26.6	26.2

<sup>a</sup>Reference 89.<sup>b</sup>Reference 96.

TABLE VI. Heat of reaction and barrier heights<sup>a</sup> (kcal/mol) for the  $\text{CH}_4 + \text{H} \leftrightarrow \text{CH}_3 + \text{H}_2$  reaction.

Level	$\Delta E$	$\Delta H_0^0$	$\Delta V_7^\ddagger$	$\Delta V_7^\ddagger$
PMP2/6-311G( <i>d,p</i> ) <sup>b</sup>	6.0	2.9	17.6(16.3)	11.6(13.4)
QCISD/6-311G( <i>d,p</i> )	2.5	-0.7	16.3(14.8)	13.8(15.5)
PMP4//UMP2 <sup>c</sup>	3.2	-0.16	15.5(14.2)	12.3(14.3)
CCSD(T)/cc-VQZ <sup>d</sup>	2.8	-0.4	15.4(13.7)	12.6(14.1)
<i>J3</i> <sup>e</sup>	2.8	-0.02	12.9(11.8)	10.1(11.9)
Expt.	2.6 <sup>f</sup>	-0.02 <sup>g</sup> , -1.3 <sup>h</sup>	(13.3 ± 0.5) <sup>h</sup>	(14.6 ± 0.4) <sup>h</sup>

<sup>a</sup>Zero-point energy corrected barriers are given in the parentheses.

<sup>b</sup>Spin projected MP2 energies at the UMP2/6-311G(*d,p*) geometries are used.

<sup>c</sup>Reference 93.

<sup>d</sup>Reference 89.

<sup>e</sup>Reference 96.

<sup>f</sup>Back calculate from the experimental heat of reaction at 0 K and harmonic frequencies taken from JANAF tables (Ref. 111).

<sup>g</sup>From JANAF tables (Ref. 111).

<sup>h</sup>Reference 114.

kcal/mol. The authors have pointed out that such a discrepancy, which also had been discussed in earlier studies,<sup>83,84</sup> is due to the scatter data in the experimental rates for the reverse reaction. Our present QCISD and the previous CCSD(T) results in fact fall within this experimental uncertainty.

The classical and zero-point energy corrected barrier heights for both the forward and reverse reactions are also given in Table VI. We found that all *ab initio* calculations yield the classical as well as zero-point energy corrected barriers noticeable higher than the values from the *J3* surface by more than 2 kcal/mol. Also, we can compare the calculated zero-point energy corrected barriers with Furue and Pacey's<sup>114</sup> experimental barriers of 13.3 and 14.6 kcal/mol for the forward and reverse reactions, respectively. The PMP2 level significantly overestimates the barrier by 3.0 kcal/mol for the forward direction while underestimating the reverse barrier by 1.2 kcal/mol, whereas the QCISD/6-311G(*d,p*) calculations overestimate the barriers for both directions by the order of 1 kcal/mol. In particular, the QCISD zero-point corrected barriers for the forward and reverse reactions are 14.8 and 15.5 kcal/mol that are also higher than the CCSD(T) barriers<sup>89</sup> by 1.1 and 1.4 kcal/mol, respectively.

In conclusion, we found that the QCISD/6-311G(*d,p*) level of theory yields geometries and vibrational frequencies at the stationary points, the reaction endoergicity and heat of reaction at 0 K for the abstraction reaction at a comparable level of accuracy with the more expensive CCSD(T)/cc-VQZ level.<sup>89</sup> The only noticeable difference in the two levels is in the calculated classical barriers. However, due to having correlation balance in the QCISD/6-311G(*d,p*) level of theory, we can scale the potential energy along the minimum energy path by a single factor to yield more accurate classical barriers for both the forward and reverse reactions. In the VTST calculations presented below, we scaled the potential along the QCISD/6-311G(*d,p*) MEP by a factor of 0.86 to match the reverse classical barrier of 11.8 kcal/mol which is the best *ab initio* estimate to date and was calculated by Kraka *et al.*<sup>89</sup> using CCSD(T)/[524p3d2 f1g/4s3p2d1f] single

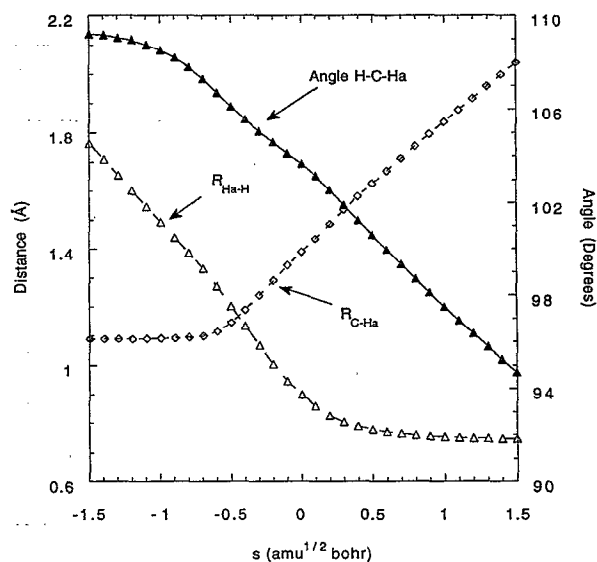


FIG. 1. Geometries along the QCISD/6-311G(*d,p*) minimum energy path for the  $\text{CH}_4 + \text{H} \leftrightarrow \text{CH}_3 + \text{H}_2$  reaction plotted vs the reaction coordinate  $s$  in the mass-weighted internal coordinates.

point energies at the optimized CCSD(T)/cc-VQZ geometries. Thus, no experimental information was used in the present dynamical calculations.

#### D. Properties along the minimum energy path

Various properties along the minimum energy path on the QCISD/6-311G(*d,p*) potential energy surface are illustrated in Figs. 1–3. Figure 1 gives the structural information along the reaction coordinate,  $s$ . Notice that the two active C–H<sub>a</sub> and H<sub>a</sub>–H bonds and the H–C–H<sub>a</sub> angle change smoothly along the reaction coordinate  $s$  indicating that the second order Gonzalez and Schelegel integration scheme yields reasonably stable MEP even with a relatively large step size, such as of 0.1 amu<sup>1/2</sup> bohr used in the present study. Figure 2 shows the classical potential energy and the ground-state vibrational adiabatic potential energy along the MEP as functions of the reaction coordinate. Comparing to the modified Valencich–Bunker–Chapman (MVBC) and the modified Raff (MR) PEF's (Fig. 1 in Ref. 98), and to the *J1*, *J2*, and *J3* PEF's (Figs. 1, 3, and 5 in Ref. 96), we found that only the MEP's from the *J1*, *J2*, and *J3* PEF's closely resemble to the present QCISD/6-311G(*d,p*) result. For more detailed discussion on the differences between these analytical PEF's, we refer readers to the two previous studies by Truhlar and co-workers.<sup>96,98</sup> The QCISD/6-311G(*d,p*) generalized transition state vibrational frequencies as functions of  $s$  are shown in Fig. 3. Again comparing the calculated generalized transition state frequencies with those from the analytical PEF's, we found that both the MVBC and MR PEF's (see Figs. 2 and 3 in Ref. 98) have many features that are noticeably different from the present *ab initio* results. The present *ab initio* generalized transition state frequencies however agree very well with those from the *J1*, *J2*, and *J3* PEF's except for the small hump near the saddle point ob-

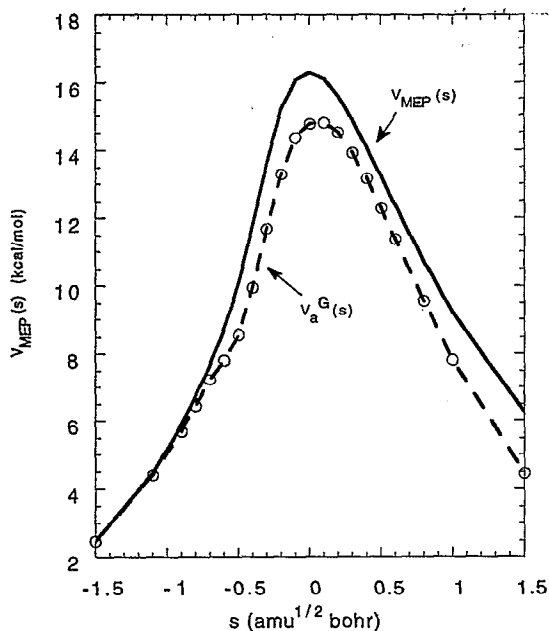


FIG. 2. The classical potential  $V_{\text{MEP}}(s)$  (solid curve) and ground-state vibrationally adiabatic potential  $V_a^G(s)$  (dashed curve) energy along the MEP as functions of the reaction coordinate  $s$ . Circles are points on the MEP where Hessian information is available.

served in these analytical PEF's for the largest generalized transition state stretching frequency (comparing Fig. 3 with Figs. 2, 4, and 6 in Ref. 96). Since the present Hessian grid is fine enough to show no such hump existed on the QCISD/6-311G( $d,p$ ) surface, we believe that this hump is an artifact in the analytical PEF's due to the functional forms used. In conclusion, except for the barrier heights, the present *ab initio* QCISD/6-311G( $d,p$ ) potential surface agrees well with

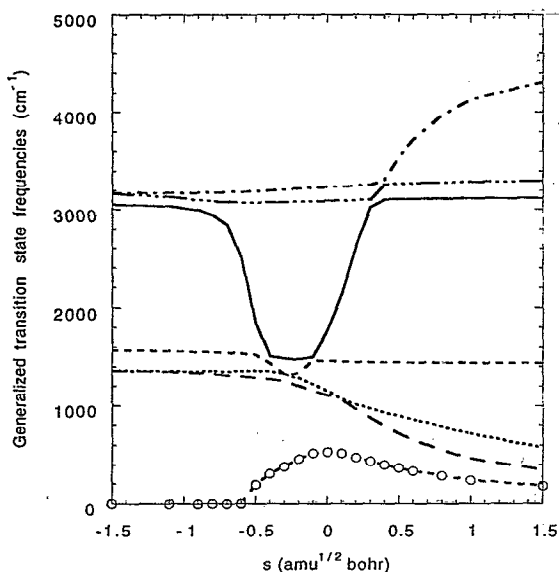


FIG. 3. Harmonic vibrational frequencies along the reaction coordinate  $s$ . Circles are points on the MEP where Hessian information is available.

the  $J3$  analytical surface which had shown to be a more accurate one among the available analytical PEF's.

### E. Rate constants

Canonical variational transition state theory (CVT) rate calculations including the centrifugal-dominant small curvature vibrationally ground-state adiabatic tunneling (SCT) contributions using the present methodology were carried out for a range of temperatures from 300 to 1500 K on the QCISD/6-311G( $d,p$ ) potential energy surface with the potential energy along the minimum energy path scaled by a factor of 0.86 for the reason mentioned earlier.

The calculated CVT/SCT forward rate constants are given in Table VII along with the previous improved CVT plus small curvature tunneling corrections (ICVT/SCSAG) rate constants<sup>96</sup> for the  $J3$  PEF, and the experimental results. The first column of experimental results in Table VII is calculated from the non-Arrhenius fit to the rate constants for the temperature range from 372 to 667 K done by Shaw.<sup>84</sup> The second column labeled as SMP is from the least-squares Arrhenius fit done by Sepehrad *et al.*<sup>85</sup> to their own data plus that of Berlie and LeRoy,<sup>60</sup> Fenimore and Jones,<sup>65</sup> and Kurylo and Timmons<sup>73</sup> over the temperature range from 400–1000 K. The third experimental column (KHT) is based on an Arrhenius fit by Kurylo, Hollinden, and Timmons.<sup>74</sup> The last experimental column is the recommended Arrhenius fit values from the most recent critical evaluation of kinetic data done by Baulch *et al.*<sup>88</sup> Note that no experimental measurements have been reported for the forward or reverse reaction below 372 K; rate constants listed in the experimental columns in Table VII for temperatures below 372 K are extrapolations based on the fits just discussed.

Agreement of the present *ab initio* CVT/SCT results with the experimental data are excellent for the wide range of temperature from 300 to 2000 K as shown in Fig. 4. More specifically, from Table VII for the temperature range from 372–667 K, experimental rate constants were very accurately measured as indicated by the small difference in the experimental data from the four different fits. In this temperature range, the agreements between our present *ab initio* CVT/SCT results with the previous ICVT/SCSAG results<sup>96</sup> from the  $J3$  analytical PEF, and with the experimental data are excellent. Though, the present CVT/SCT rate constants are slightly larger than the experimental data but within the experimental deviations from different fits, and are closer to the recent recommended values of Baulch *et al.*<sup>88</sup> with the maximum deviation factor of 1.2 at 372 K. At temperatures below 372 K where no experimental measurements were available, our *ab initio* CVT/SCT results agree very well with the results from the  $J3$  surface, however, both are somewhat larger than the extrapolations from the experimental fits. For temperatures above 667 K, we found that the present *ab initio* results are in excellent agreement with the recent Baulch *et al.*'s recommended values with the maximum deviation factor of 1.2 at 1340 K. However, both are noticeably larger than the ICVT/SCSAG rate constants<sup>96</sup> from the  $J3$  surface, and experimental values from Shaw<sup>84</sup> and from Sepehrad *et al.*<sup>85</sup> (SMP) with the maximum deviation factor of 2.6. Note that among the experimental data, the

TABLE VII. Rate constants ( $\text{cm}^3 \text{ molecule}^{-1} \text{ s}^{-1}$ ) for the reaction  $\text{CH}_4 + \text{H} \rightarrow \text{CH}_3 + \text{H}_2$ .<sup>a</sup>

$T$ (K)	QCISD <sup>b</sup>	$J3$ <sup>c</sup>	Shaw <sup>d</sup>	SMP <sup>e</sup>	KTH <sup>f</sup>	Baulch <i>et al.</i> <sup>g</sup>
298	1.3E-18	9.9E-19	[6.8E-19]	[2.2E-19]	[3.2E-19]	[7.4E-19]
300	1.4E-18	1.1E-18	[7.6E-19]	[2.5E-19]	[3.7E-19]	[8.2E-19]
372	2.6E-17	2.3E-17	2.1E-17	[1.2E-17]	1.6E-17	2.1E-17
400	6.6E-17	6.0E-17	5.6E-17	3.8E-17	4.8E-17	5.7E-17
424	1.4E-16	1.2E-16	1.2E-16	8.8E-17	1.1E-16	1.2E-16
500	9.3E-16	8.0E-16	8.0E-16	7.6E-16	8.8E-16	8.4E-16
600	6.3E-15	5.0E-15	5.1E-15	5.6E-15	6.2E-15	5.6E-15
667	1.7E-14	1.3E-14	1.3E-14	1.5E-14	1.6E-14	1.5E-14
1000	4.7E-13	2.9E-13	[2.7E-13]	3.1E-13	...	3.8E-13
1340	3.1E-12	1.8E-12	[1.5E-12]	1.4E-12	...	2.6E-12
1500	5.9E-12	3.2E-12	[2.7E-12]	2.3E-12	...	5.0E-12

<sup>a</sup>Values in brackets are extrapolations.

<sup>b</sup>The present CVT/SCT results at the QCISD/6-311G(*d,p*) level with the  $V_{\text{MEP}}$  scaled by a factor of 0.86.

<sup>c</sup>Previous ICVT/SCSAG results from the  $J3$  semiempirical PEF (Ref. 96).

<sup>d</sup>Non-Arrhenius fit by Shaw (Ref. 84).

<sup>e</sup>Best Arrhenius fit of published data in the range 400–1800 K as determined by Sepehrad *et al.* (Ref. 85).

<sup>f</sup>Arrhenius fit of Kurylo *et al.* (Ref. 74).

<sup>g</sup>Most recently recommended values from the Arrhenius fit of Baulch *et al.* (Ref. 88).

Baulch *et al.*'s values are more accurate in the high temperature region since they are from a better fit to the high temperature data.<sup>88</sup>

The reverse rate constants including the present *ab initio* CVT/SCT results, the previous ICVT/SCSAG rate constants<sup>96</sup> from the  $J3$  surface, and the experimental data from various fits are summarized in Table VIII. The experimental results by Shaw<sup>84</sup> and Sepehrad *et al.*<sup>85</sup> in the first

two experimental columns both are computed using their fits for the forward rate constants and the corresponding JANAF equilibrium constants.<sup>111</sup> The third experimental column is based on an Arrhenius fit by Kerr and Parsonage<sup>83</sup> (KP) using a critical analysis of the experimental data for the reverse reaction. Similarly, the last column is from a recent Arrhenius fit done by Baulch *et al.*<sup>88</sup> which included the more recent high temperature measurements. Notice that there is a good agreement between data obtained from the forward rates and the equilibrium constants by Shaw<sup>84</sup> and Sepahrad *et al.*,<sup>85</sup> and between data obtained from the Arrhenius fits to the measured rates by Kerr and Parsonage<sup>83</sup> and by Baulch *et al.*<sup>88</sup> However, there is a large deviation in the experimental data between these two groups representing different ways of obtaining the reverse rate constants. Data from those Shaw<sup>84</sup> and SMP (Ref. 85) are noticeably larger than those from the other two with the maximum deviation factor of 7.3 at 372 K between the fits from Shaw<sup>84</sup> and Baulch *et al.*<sup>88</sup>

The Arrhenius plot of the calculated and experimental rate constants shown in Fig. 5 indicates good agreement between the calculated *ab initio* rate constants and available experimental measurements for a wide range of temperature. More specifically, in comparison with the experimental data from different fits, we found that the present *ab initio* results are within the range of the experimental uncertainty. Though, they agree slightly better with the experimental data obtained from the fits by KP (Ref. 83) and Baulch *et al.*<sup>88</sup> than from the fits by Shaw<sup>84</sup> and SMP.<sup>85</sup> The ICVT/SCSAG results<sup>96</sup> from the  $J3$  PEF on the other hand agree very well with the fit from Shaw,<sup>84</sup> though this is expected since the  $J3$  PEF (Ref. 96) was calibrated to the equilibrium constants from the JANAF tables<sup>111</sup> and the experimental forward rate constant at 667 K. It is also important to point out that the vibrational partition functions in the present CVT calculations were calculated within the harmonic approximation. Anharmonicity can be important particularly for low real frequency modes such as the doubly degenerate bend mode of the generalize transition state. Including anharmonicity cor-

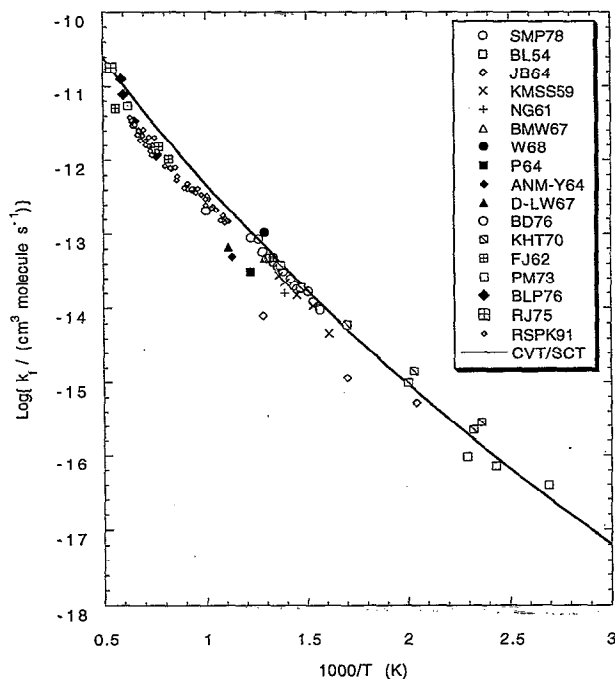


FIG. 4. Arrhenius plot of the forward rate constants vs  $1/T$ . The solid curve is the present CVT/SCT results; SMP78, Ref. 85; BI54, Ref. 60; JB64, Ref. 68; KMSS59, Ref. 63; NG61, Ref. 66; BMW67, Ref. 70; W68, Ref. 72; P64, Ref. 69; ANM-Y64, Ref. 67; D-LW67, Ref. 71; BD76, Ref. 82; KTH70, Ref. 74; FJ62, Ref. 65; PM73, Ref. 77; BLP76, Ref. 81; RJ75, Ref. 80; RSPK91, Ref. 87.

TABLE VIII. Rate constants ( $\text{cm}^3 \text{ molecule}^{-1} \text{ s}^{-1}$ ) for the reaction  $\text{CH}_3 + \text{H}_2 \rightarrow \text{CH}_4 + \text{H}$ .<sup>a</sup>

$T$ (K)	QCISD <sup>b</sup>	$J3$ <sup>c</sup>	Shaw <sup>d</sup>	SMP <sup>e</sup>	KP <sup>f</sup>	Baulch <i>et al.</i> <sup>g</sup>
298	5.2E-20	1.7E-19	[1.1E-19]	[3.5E-20]	[1.4E-20]	[8.5E-21]
300	5.7E-20	1.9E-19	[1.2E-19]	[4.0E-20]	[1.6E-20]	[9.6E-21]
372	1.1E-18	3.2E-18	2.7E-18	[1.6E-18]	5.6E-19	3.7E-19
400	2.6E-18	7.4E-18	6.5E-18	4.4E-18	1.6E-18	1.1E-18
424	5.3E-18	1.4E-17	1.3E-17	9.7E-18	3.4E-18	2.5E-18
500	3.4E-17	7.6E-17	7.3E-17	6.9E-17	2.4E-17	2.2E-17
600	2.1E-16	3.9E-16	3.8E-16	4.2E-16	1.5E-16	1.7E-16
667	5.4E-16	9.1E-16	9.0E-16	1.0E-15	3.8E-16	5.1E-16
1000	1.2E-14	1.4E-14	[1.3E-14]	1.5E-14	...	1.7E-14
1340	7.6E-14	7.5E-14	[6.6E-14]	6.1E-14	...	1.2E-13
1500	1.4E-13	1.4E-13	[1.1E-13]	9.4E-14	...	2.4E-13

<sup>a</sup>Values in brackets are extrapolations.<sup>b</sup>The present CVT/SCT results at the QCISD/6-311G( $d,p$ ) level with the  $V_{\text{MEP}}$  scaled by a factor of 0.86.<sup>c</sup>Previous ICVT/SCSAG results from the semiempirical  $J3$  PEF (Ref. 95).<sup>d</sup>Computed from forward rate constants of Ref. 84 and JANAF equilibrium constants (Ref. 110).<sup>e</sup>Computed from forward rate constants of Ref. 74 and JANAF equilibrium constants (Ref. 110).<sup>f</sup>Computed from the Arrhenius fit of Ref. 83.<sup>g</sup>Most recently recommended values from the Arrhenius fit of Baulch *et al.* (Ref. 87).

reaction for this mode was found to decrease the rate constants in the previous ICVT/SCSAG calculations,<sup>96</sup> thus it would make the present CVT/SCT results even in better agreement with those from Baulch *et al.*<sup>88</sup>

## V. CONCLUSION

We have presented a new methodology for direct *ab initio* dynamics calculations of thermal rate constants from first principles. This method is based on a variational transition state theory plus multidimensional semiclassical tunneling corrections within the framework of the small-curvature approximation with the potential energy information to be calculated from a sufficiently accurate level of electronic structure theory. We have applied the new method to study detailed dynamics of the hydrogen abstraction of methane by hydrogen atom,  $\text{CH}_4 + \text{H} \leftrightarrow \text{CH}_3 + \text{H}_2$ , and obtained excellent agreement with the available experimental data for both the forward and reverse rate constants for a wide range of temperature from 300 to 1500 K.

In particular, for application to the  $\text{CH}_4 + \text{H} \leftrightarrow \text{CH}_3 + \text{H}_2$  reaction, we found that the QCISD level of theory provides a well balance in the treatment electron correlation in the  $\text{H}_3\text{C}-\text{H}$  and  $\text{H}-\text{H}$  bonds, as a result it yields more accurate reaction energetics for the abstraction reaction than the MP2 or MP4 level. Furthermore, the QCISD/6-311G( $d,p$ ) level of theory predicts geometries and harmonic frequencies with comparable accuracy to the more expensive CCSD(T)/[5s4p3d/4s3p] level of theory. The only noticeable difference between these two levels is in the calculated classical barriers. Particularly, the present QCISD/6-311G( $d,p$ ) calculations yield the forward and reverse classical barriers about 1 kcal/mol higher than the previous CCSD(T)/[5s4p3d/4s3p] calculations. However, for the CVT/SCT rate calculations, we can take into account the error in the QCISD classical barrier heights by scaling the potential energy along the minimum energy path by a factor of 0.86 to match the more accurate classical barrier height which was calculated from the CCSD(T) single point calculations by Kraka *et al.*<sup>89</sup> using the [5s4p3d2 f1g/4s3p2d1f] basis set at the CCSD(T)/[5s4p3d/4s3p] geometries. Finally, the calculated *ab initio* CVT/SCT rate constants for the forward and

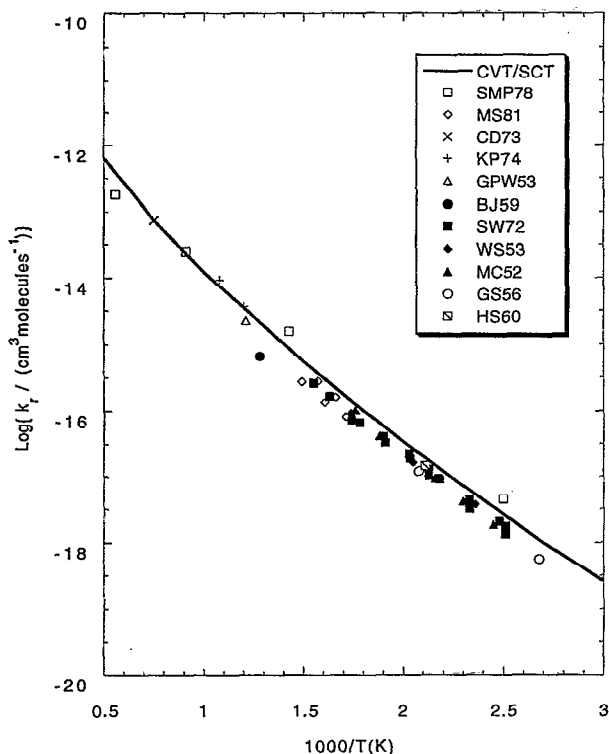


FIG. 5. Arrhenius plot of the reverse rate constants vs  $1/T$ . The solid curve is the present CVT/SCT results. SMP78, Ref. 85; MS81, Ref. 86; CD73, Ref. 76; KP74, Ref. 78; GPW53, Ref. 58; BJ59, Ref. 62; SW72, Ref. 75; WS53, Ref. 59; MC52, Ref. 57; GS56, Ref. 61; HS60, Ref. 64.

TABLE IX. Total energies (hartree).

Level/basis	CH <sub>4</sub>	CH <sub>3</sub>	H <sub>2</sub>	H <sup>a</sup>	CH <sub>5</sub> TS
MP2/6-311G(d,p) <sup>b</sup>	-40.379 23	-39.707 24	-1.160 27	-0.499 81	-40.846 08
		-39.709 17			-40.850 97
MP2/cc-pVDZ <sup>b</sup>	-40.367 73	-39.698 27	-1.156 21	-0.499 33	-40.835 45
		-39.700 17			-40.840 34
QCISD/6-311G(d,p)	-40.401 64	-39.729 16	-1.168 34	-0.499 81	-40.875 50
QCISD/cc-pVDZ	-40.391 41	-39.721 47	-1.164 90	-0.499 33	-40.866 86

<sup>a</sup>Calculated at the UHF level.<sup>b</sup>The first line is without spin projection (UMP2) and the second line is with spin projection PMP2/6-311G(d,p) at the UMP2 geometries.

reverse reactions agree very well with the experimental data within the experimental uncertainty for a wide range of temperatures. In addition, the QCISD/6-311G(d,p) generalized transition state vibrational frequencies also provide information to examine unusual features on the analytical potential energy functions that otherwise would not be possible.

We conclude that the present direct *ab initio* dynamics method provides a powerful and practical tool for modeling detailed quantum dynamics and elucidating reaction mechanisms from first principles for chemical reactions involving small polyatomic molecules. Application of this method to study the kinetic isotope effects for the CH<sub>4</sub>+H↔CH<sub>3</sub>+H<sub>2</sub> reaction is now in progress.

## ACKNOWLEDGMENTS

This work was supported in part by the University of Utah, and the National Science Foundation through a NSF Postdoctoral Fellowship Startup Grant. T.N.T. is a recipient of a 1993 NSF Young Investigator Award.

## APPENDIX

Table IX is presented as supplementary to material.

- <sup>1</sup>I. Wang and M. J. Karplus, *J. Am. Chem. Soc.* **95**, 8160 (1973).
- <sup>2</sup>D. Malcome-Lawes, *J. Am. Chem. Soc. Faraday Trans. 2* **71**, 1183 (1975).
- <sup>3</sup>A. Warshel and M. Karplus, *Chem. Phys. Lett.* **32**, 11 (1975).
- <sup>4</sup>S. K. Gray, W. H. Miller, Y. Yamaguchi, and H. F. Schaefer, *J. Am. Chem. Soc.* **103**, 1900 (1981).
- <sup>5</sup>K. Moroduma and S. Kato, in *Potential Energy Surfaces and Dynamics Calculations* (Plenum, New York, 1981), pp. 243–264.
- <sup>6</sup>D. G. Truhlar, J. W. Duff, N. C. Blais, J. C. Tully, and B. C. Garrett, *J. Chem. Phys.* **77**, 764 (1982).
- <sup>7</sup>R. Car and M. Parrinello, *Phys. Rev. Lett.* **55**, 2471 (1985).
- <sup>8</sup>S. M. Colwell and N. C. Handy, *J. Chem. Phys.* **82**, 1281 (1985).
- <sup>9</sup>A. Tachibana, I. Okazaki, M. Koizumi, K. Hori, and T. Yamabe, *J. Am. Chem. Soc.* **107**, 1190 (1985).
- <sup>10</sup>A. Tachibana, H. Fueno, and T. Yamabe, *J. Am. Chem. Soc.* **108**, 4346 (1986).
- <sup>11</sup>D. G. Truhlar, M. S. Gordon, and R. Steckler, *Chem. Rev.* **87**, 217 (1987).
- <sup>12</sup>C. J. Doubleday, J. W. J. McIver, and M. Page, *J. Phys. Chem.* **92**, 4367 (1988).
- <sup>13</sup>K. K. Baldridge, M. S. Gordon, D. G. Truhlar, and R. Steckler, *J. Phys. Chem.* **93**, 5107 (1989).
- <sup>14</sup>R. Car and M. Parrinello, in *Simple Molecular Systems at Very High Density*, edited by A. Polian, P. Loubeyre, and N. Boccara (Plenum, New York, 1989), p. 455.
- <sup>15</sup>M. J. Field, *Chem. Phys. Lett.* **172**, 83 (1990).
- <sup>16</sup>B. C. Garrett, M. L. Koszykowski, C. F. Melius, and M. Page, *J. Phys. Chem.* **94**, 7096 (1990).
- <sup>17</sup>T. Helgaker, E. Uggerud, and H. J. A. Jensen, *Chem. Phys. Lett.* **173**, 145 (1990).
- <sup>18</sup>D. Remler and P. A. Madden, *Mol. Phys.* **70**, 921 (1990).
- <sup>19</sup>D. G. Truhlar and M. S. Gordon, *Science* **249**, 491 (1990).
- <sup>20</sup>T. N. Truong and D. G. Truhlar, *J. Chem. Phys.* **93**, 1761 (1990).
- <sup>21</sup>B. C. Garrett, C. F. Melius, and M. Page, in *Theoretical and Computational Models for Organic Chemistry*, edited by S. J. Formosinho, I. G. Csizmadia, and L. G. Arnaut (Kluwer, Dordrecht, 1991), pp. 25–54.
- <sup>22</sup>A. Gonzalez-Lafont, T. N. Truong, and D. G. Truhlar, *J. Phys. Chem.* **95**, 4618 (1991).
- <sup>23</sup>A. Gonzalez-Lafont, T. N. Truong, and D. G. Truhlar, *J. Chem. Phys.* **95**, 8875 (1991).
- <sup>24</sup>T. N. Truong and J. A. McCammon, *J. Am. Chem. Soc.* **113**, 7504 (1991).
- <sup>25</sup>A. A. Viggiano, J. Paschekewitz, R. A. Morris, J. F. Paulson, A. Gonzalez-Lafont, and D. G. Truhlar, *J. Am. Chem. Soc.* **113**, 9404 (1991).
- <sup>26</sup>B. Hartke and E. A. Carter, *J. Chem. Phys.* **97**, 6569 (1992).
- <sup>27</sup>E. Uggerud and T. Helgaker, *J. Am. Chem. Soc.* **114**, 4265 (1992).
- <sup>28</sup>Y.-P. Liu, D.-h. Lu, A. Gonzalez-Lafont, D. G. Truhlar, and B. C. Garrett, *J. Am. Chem. Soc.* **115**, 7806 (1993).
- <sup>29</sup>Y.-P. Liu, G. C. Lynch, T. N. Truong, D.-h. Lu, and D. G. Truhlar, *J. Am. Chem. Soc.* **115**, 2408 (1993).
- <sup>30</sup>D. G. Truhlar, A. D. Isaacson, R. T. Skodje, and B. C. Garrett, *J. Phys. Chem.* **86**, 2252 (1982).
- <sup>31</sup>D. G. Truhlar and B. C. Garrett, *Annu. Rev. Phys. Chem.* **35**, 159 (1984).
- <sup>32</sup>D. G. Truhlar, A. D. Isaacson, and B. C. Garrett, in *Theory of Chemical Reaction Dynamics*, edited by M. Baer (Chemical Rubber, Boca Raton, FL, 1985), Vol. 4, pp. 65–137.
- <sup>33</sup>D. G. Truhlar and B. C. Garrett, *J. Chem. Phys.* **84**, 365 (1987).
- <sup>34</sup>S. C. Tucker and D. G. Truhlar, in *New Theoretical Concepts for Understanding Organic Reactions*, edited by J. Bertran and I. G. Csizmadia (Kluwer, Dordrecht, Netherlands, 1989), pp. 291–346.
- <sup>35</sup>D.-h. Lu, T. N. Truong, V. S. Melissas, G. C. Lynch, Y. P. Liu, B. C. Garrett, R. Steckler, A. D. Isaacson, S. N. Rai, G. C. Hancock, J. G. Lauderdale, T. Joseph, and D. G. Truhlar, *Comput. Phys. Commun.* **71**, 235 (1992).
- <sup>36</sup>J. A. Pople, D. P. Santry, and G. A. Segal, *J. Chem. Phys.* **43**, S129 (1965).
- <sup>37</sup>M. J. S. Dewar and W. Thiel, *J. Am. Chem. Soc.* **99**, 4899 (1977).
- <sup>38</sup>J. J. P. Stewart, *J. Comput. Aided Mol. Design* **4**, 48 (1990).
- <sup>39</sup>E. Wigner, *J. Chem. Phys.* **5**, 720 (1937).
- <sup>40</sup>J. Horiuti, *Bull. Chem. Soc. Jpn.* **13**, 210 (1938).
- <sup>41</sup>M. A. Eliason and J. O. Hirshfelder, *J. Chem. Phys.* **30**, 1426 (1959).
- <sup>42</sup>J. C. Keck, *J. Chem. Phys.* **32**, 1035 (1960).
- <sup>43</sup>J. C. Keck, *Adv. Chem. Phys.* **13**, 85 (1967).
- <sup>44</sup>M. Quack and J. Troe, *Ber. Bunsenges. Phys. Chem.* **81**, 329 (1977).
- <sup>45</sup>M. Quack and J. Troe, *Chem. Soc. Spec. Per. Rep. Gas Kinet. Energy Trans.* **2**, 175 (1977).
- <sup>46</sup>B. C. Garrett and D. G. Truhlar, *J. Chem. Phys.* **70**, 1593 (1979).
- <sup>47</sup>D. G. Truhlar and B. C. Garrett, *Acc. Chem. Res.* **13**, 440 (1980).
- <sup>48</sup>P. Pechukas, *Annu. Rev. Phys. Chem.* **32**, 159 (1981).
- <sup>49</sup>W. J. Chesnavich and M. T. Bowers, *Prog. React. Kinet.* **11**, 137 (1982).
- <sup>50</sup>D. L. Martin and L. M. Raff, *J. Chem. Phys.* **77**, 1235 (1982).
- <sup>51</sup>W. L. Hase, *Acc. Chem. Res.* **16**, 258 (1983).
- <sup>52</sup>W. J. Chesnavich, *Chem. Phys.* **84**, 2615 (1986).
- <sup>53</sup>S. J. Klippenstein and R. A. Marcus, *J. Chem. Phys.* **87**, 3410 (1987).
- <sup>54</sup>D. I. Sverdlik and G. W. Koeppl, *J. Chem. Phys.* **91**, 250 (1989).

- <sup>55</sup>J. Warnatz, in *Combustion Chemistry*, edited by W. C. Gardiner, Jr. (Springer, New York, 1984), p. 233.
- <sup>56</sup>D. J. Hucknall, *Chemistry of Hydrocarbons* (Chapman and Hall, London, 1985).
- <sup>57</sup>T. G. Majury and E. W. R. Steacie, *J. Chem. Phys.* **20**, 197 (1952).
- <sup>58</sup>B. G. Gowenlock, J. C. Polanyi, and E. Warhurst, *Proc. R. Soc. London Ser. A* **218**, 269 (1953).
- <sup>59</sup>E. Whittle and E. W. R. Steacie, *J. Chem. Phys.* **21**, 993 (1953).
- <sup>60</sup>M. R. Berlie and D. J. Le Roy, *Can. J. Chem.* **32**, 650 (1954).
- <sup>61</sup>H. Gesser and E. W. R. Steacie, *Can. J. Chem.* **34**, 113 (1956).
- <sup>62</sup>S. W. Benson and D. V. S. Jain, *J. Chem. Phys.* **31**, 1008 (1959).
- <sup>63</sup>R. Klein, J. R. McNesby, M. D. Scheer, and L. J. Schoen, *J. Chem. Phys.* **30**, 58 (1959).
- <sup>64</sup>J. F. Henderson and E. W. R. Steacie, *Can. J. Chem.* **38**, 2161 (1960).
- <sup>65</sup>C. P. Fenimore and G. W. Jones, *J. Phys. Chem.* **65**, 2200 (1961).
- <sup>66</sup>A. B. Nalbandyan and N. I. Gorban, *Akad. Nauk Ar. SSR Dokl.* **33**, 49 (1961).
- <sup>67</sup>V. V. Azatyán, A. B. Nalbandyan, and T. Meng-Yuan, *Kinet. Catal.* **5**, 177 (1964).
- <sup>68</sup>J. W. S. Jamieson and G. R. Brown, *Can. J. Chem.* **42**, 1638 (1964).
- <sup>69</sup>B. N. Panfilov, Author's summary of Dissertation, Siberian Section, Acad. Sci USSR Novosibirsk, 1964.
- <sup>70</sup>R. R. Baldwin, A. C. Morris, and R. W. Walker, *Proceedings of the 11th International Symposium on Combustion* (Combustion Institute, Pittsburgh, 1967), p. 889.
- <sup>71</sup>G. Dixon-Lewis and A. Williams, *Proceedings of the 11th International Symposium on Combustion* (Combustion Institute, Pittsburgh, 1967), p. 951.
- <sup>72</sup>R. W. Walker, *J. Chem. Soc. A* **1968**, 2391.
- <sup>73</sup>M. J. Kurylo and R. B. Timmons, *J. Chem. Phys.* **50**, 5076 (1969).
- <sup>74</sup>M. J. Kurylo, G. A. Hollinden, and R. B. Timmons, *J. Chem. Phys.* **52**, 1773 (1970).
- <sup>75</sup>J. S. Shapiro and R. E. Weston, Jr., *J. Phys. Chem.* **76**, 1669 (1972).
- <sup>76</sup>T. C. Clark and J. E. Dove, *Can. J. Chem.* **51**, 2155 (1973).
- <sup>77</sup>J. Peeters and G. Mahnen, in *Proceedings of the 14th International Symposium on Combustion* (The Combustion Institute, Pittsburgh, 1973), p. 133.
- <sup>78</sup>P. C. Kobrinsky and P. D. Pacey, *Can. J. Chem.* **52**, 3665 (1974).
- <sup>79</sup>S. W. Benson, D. M. Golden, R. W. Lawrence, R. Shawe, and R. W. Woolfolk, *Int. J. Chem. Kin. Symp.* **1**, 399 (1975).
- <sup>80</sup>P. Roth and T. Just, *Ber. Bunsenges.* **79**, 682 (1975).
- <sup>81</sup>J. C. Biorci, C. P. Lazzara, and J. F. Papp, *Combust. Flame* **26**, 57 (1976).
- <sup>82</sup>S. F. Bush and P. Dyer, *Proc. R. Soc. London Ser. A* **351**, 33 (1976).
- <sup>83</sup>J. A. Kerr and M. J. Parsonage, *Evaluated Kinetic Data on Gas Phase Hydrogen Transfer Reactions of Methyl Radicals* (Butterworths, London, 1976).
- <sup>84</sup>R. Shaw, *J. Phys. Chem. Ref. Data* **7**, 1179 (1978).
- <sup>85</sup>A. Sepéhrad, R. M. Marshall, and H. Purnell, *J. Chem. Soc. Faraday Trans. 1* **75**, 835 (1979).
- <sup>86</sup>R. M. Marshall and G. Shahkar, *J. Chem. Soc. Faraday Trans. I* **77**, 2271 (1981).
- <sup>87</sup>M. J. Rabinowitz, J. W. Sutherland, P. M. Patterson, and R. B. Klemm, *J. Phys. Chem.* **95**, 674 (1991).
- <sup>88</sup>D. L. Baulch, C. J. Cobos, R. A. Cox, Esser, P. Frank, T. Just, J. A. Kerr, M. J. Pilling, J. Troe, R. W. Walker, and J. Warnatz, *J. Phys. Chem. Ref. Data* **21**, 441 (1992).
- <sup>89</sup>E. Kraka, J. Gauss, and D. Cremer, *J. Chem. Phys.* **99**, 5306 (1993).
- <sup>90</sup>G. C. Schatz, S. P. Walch, and A. F. Wagner, *J. Chem. Phys.* **73**, 4536 (1980).
- <sup>91</sup>S. P. Walch, *J. Chem. Phys.* **72**, 4932 (1980).
- <sup>92</sup>G. C. Schatz, A. F. Wagner, and T. H. Dunning, Jr., *J. Phys. Chem.* **88**, 221 (1984).
- <sup>93</sup>C. Gonzalez, J. J. W. McDoual, and H. B. Schlegel, *J. Phys. Chem.* **94**, 7467 (1990).
- <sup>94</sup>L. M. Raff, *J. Chem. Phys.* **60**, 2220 (1974).
- <sup>95</sup>S. Chapman and D. L. Bunker, *J. Chem. Phys.* **62**, 2890 (1975).
- <sup>96</sup>T. Joseph, R. Steckler, and D. G. Truhlar, *J. Chem. Phys.* **87**, 7036 (1987).
- <sup>97</sup>D. H. Lu, D. Maurice, and D. G. Truhlar, *J. Am. Chem. Soc.* **112**, 6206 (1990).
- <sup>98</sup>R. Steckler, F. B. Brown, K. J. Dykema, G. C. Hancock, D. G. Truhlar, and T. Valencich, *J. Chem. Phys.* **87**, 7024 (1987).
- <sup>99</sup>J. A. Pople, M. Head-Gordon, and K. Raghavachari, *J. Chem. Phys.* **87**, 5968 (1987).
- <sup>100</sup>R. Krishnan, J. S. Binkley, R. Seeger, and J. A. Pople, *J. Chem. Phys.* **72**, 650 (1980).
- <sup>101</sup>B. C. Garrett, N. Abushalbi, D. J. Kouri, and D. G. Truhlar, *J. Chem. Phys.* **83**, 2252 (1985).
- <sup>102</sup>M. M. Kreevoy, D. Ostovic, D. G. Truhlar, and B. C. Garrett, *J. Phys. Chem.* **90**, 3766 (1986).
- <sup>103</sup>A. D. Isaacson, B. C. Garrett, G. C. Hancock, S. N. Rai, M. J. Redmon, R. Steckler, and D. G. Truhlar, *Comput. Phys. Commun.* **47**, 91 (1987).
- <sup>104</sup>B. C. Garrett, T. Joseph, T. N. Truong, and D. G. Truhlar, *Chem. Phys.* **136**, 271 (1989).
- <sup>105</sup>M. Page and J. W. McIver, Jr., *J. Chem. Phys.* **88**, 922 (1988).
- <sup>106</sup>C. Möller and M. S. Plesset, *Phys. Rev.* **46**, 618 (1934).
- <sup>107</sup>T. H. Dunning, Jr., *J. Chem. Phys.* **90**, 1007 (1989).
- <sup>108</sup>C. Gonzalez and H. B. Schlegel, *J. Phys. Chem.* **94**, 5523 (1990).
- <sup>109</sup>M. J. Frisch, G. W. Trucks, M. Head-Gordon, P. M. W. Gill, M. W. Wong, J. B. Foresman, B. G. Johnson, H. B. Schlegel, M. A. Robb, E. S. Replogle, R. Gomperts, J. L. Andres, K. Raghavachari, J. S. Binkley, C. Gonzalez, R. L. Martin, D. J. Fox, D. J. Defrees, J. Baker, J. J. P. Stewart, and J. A. Pople, GAUSSIAN 92, Gaussian, Inc., Pittsburgh, Pennsylvania, 1992.
- <sup>110</sup>T. N. Truong, DIRATE (unpublished), University of Utah, Salt Lake City, Utah, 1993.
- <sup>111</sup>JANAF Thermochemical Tables (U.S. GPO, Washington, DC, 1971), Vol. 37.
- <sup>112</sup>K. P. Huber and G. Herzberg, *Constants of Diatomic Molecules* (Van Nostrand Reinhold, New York, 1979).
- <sup>113</sup>M. S. Gordon and D. G. Truhlar, *J. Am. Chem. Soc.* **108**, 5412 (1986).
- <sup>114</sup>H. Furue and P. D. Pacey, *J. Phys. Chem.* **94**, 1419 (1990).